Biochimica et Biophysica Acta 893 (1987) 126–137
Elsevier

BBA 42577

Light-induced oxidation of the acceptor-side Fe(II) of Photosystem II by exogenous quinones acting through the Q_B binding site. I. Quinones, kinetics and pH-dependence

Vasili Petrouleas [a] and Bruce A. Diner [b]

[a] *Nuclear Research Center 'Demokritos', Athens (Greece) and* [b] *Institut de Biologie Physico-Chimique, Paris (France)*

(Received 7 November 1986)
(Revised manuscript received 7 May 1987)

Key words: Electron spin resonance; Photosystem II; Quinone-iron acceptor complex; Q_{400}; Reduction-induced oxidation; Benzoquinone

We have recently shown by optical, EPR and Mössbauer spectroscopy that the high spin Fe(II) of the quinone-iron acceptor complex of Photosystem II can be oxidized by ferricyanide to high-spin Fe(III). The midpoint potential of the Fe(III)/Fe(II) couple is 370 mV at pH 7.5 and shows an approximate pH-dependence of −60 mV/pH unit. The iron was identified as being responsible for the high potential Photosystem II acceptor known as Q_{400}, discovered by Ikegami and Katoh ((1975) Plant Cell Physiol. 14, 829–836) but until now not identified chemically. We establish here that Q_A and the oxidized Fe(III) are linked in series, with Q_A the first to be reduced in the primary charge separation of Photosystem II. At pH 7.5, an electron is then transferred from Q_A^- to Fe(III) with a $t_{1/2}$ of 25 μs, reforming Q_AFe(II). The Fe(II) can also be oxidized to Fe(III) in oxygen-evolving thylakoid membranes through a photoreduction-induced oxidation in the presence of exogenous quinones, where $E_{m,7}(Q^-/QH_2) > E_{m,7}(Fe(III)/Fe(II)) - 60$ mV. Single turnover illumination of the Photosystem II reaction center at 200 K, followed by warming to 0 °C, results in photoreduction of these quinones to the semiquinone form which in turn oxidizes the Fe(II) to Fe(III). A second turnover of the reaction center reduces Fe(III) back to Fe(II). These reactions, similar to those reported by Zimmermann and Rutherford (Zimmermann, J.L. and Rutherford, A.W. (1986) Biochim. Biophys. Acta 851, 416–423) at room temperature, in work largely done in parallel, are summarized below:

$$Q_A Fe(II) \xrightarrow[200\ K]{h\nu} Q_A^- Fe(II) \underset{0\,^\circ C}{\overset{Q_{ex}}{\leftrightarrow}} Q_A Fe(II) Q_{ex}^- \underset{0\,^\circ C}{\overset{2H^+}{\leftrightarrow}} Q_A Fe(III) Q_{ex} H_2$$

$$Q_A Fe(III) \xrightarrow[200\ K]{h\nu} Q_A^- Fe(III) \underset{200\ K}{\leftrightarrow} Q_A Fe(II)$$

Abbreviations: BBY, Berthold, Babcock and Yocum (see Ref. 17); Ches, 2-[*N*-cyclohexylamino]ethanesulfonic acid; Chl, chlorophyll; DCMU, diuron (3-(3,4-dichlorophenyl)-1,1-dimethylurea); EDTA, ethylenediaminetetraacetate; Hepes, 4-(2-hydroxyethyl)-1-piperazineethanesulfonic acid; Mes, 4-morpholineethanesulfonic acid; *p*-BQ, 1,4-benzoquinone; PQ-1, plastoquinone-1; PQ-9, plastoquinone *a*; PS II, Photosystem II; RC, reaction center; Q_A, primary quinone electron acceptor; Q_B, secondary quinone electron acceptor; Q_{ex}, exogenous quinone; UQ-1, ubiquinone-1.

Correspondence: B.A. Diner, (present address:) Central Research and Development Department, Experimental Station E402/2224, E.I. du Pont de Nemours & Co. Inc., Wilmington, DE 19898, U.S.A.

where Q_A and Q_{ex} are the primary quinone acceptor of Photosystem II and exogenous quinone, respectively. Detection of Fe(III) at $g = 8$ by EPR spectroscopy shows this signal to oscillate with period two upon successive turnovers of the Photosystem II reaction center. Different exogenous quinones give different EPR spectra for Fe(III), indicating that these bind close to the Fe binding site and modify the symmetry of the Fe(III) environment. A study of the pH-dependence of the light-induced oxidation of the Fe(III) by phenyl-*p*-BQ shows a pH-optimum at 6–7. The decline at higher pH is consistent with a pH-dependence of -60 mV/pH unit and -120 mV/pH unit, respectively, for redox couples Fe(III)/Fe(II) and Q^-/QH_2. The decline at lower pH was not foreseen and appears associated with a transformation of the quinone-iron environment from that showing a Q_A^-Fe(II) EPR resonance of $g = 1.9$ at high pH to one at $g = 1.84$ below pH 6.5. The latter form appears not to support light-induced oxidation of the Fe(II) by exogenous quinones.

Introduction

The reaction center of Photosystem II contains two plastoquinone electron acceptors, Q_A and Q_B. Q_A receives an electron from a reduced pheophytin within 250–300 ps [1] of the primary charge separation. Q_A^- then transfers an electron to Q_B with a half-time of 0.2 ms [2]. A second charge separation again produces Q_A^- which transfers its electron to $Q_B^-(H^+)$ [3]. This electron transfer is coupled to the binding of two protons, producing the quinol, Q_BH_2. If we assume analogy with the photosynthetic bacteria, the two quinones are located close to (probably within 7 Å), but not coordinated to [4–6] a high spin ($S = 2$) Fe(II) [7]. This close proximity is revealed by magnetic coupling between the Fe(II) and the paramagnetic semiquinone forms of Q_A and Q_B [8,9].

We have recently shown [10] that the Fe(II) can be oxidized by ferricyanide to high spin ($S = 5/2$) Fe(III). The midpoint potential ($E_{m,7.5} = 370$ mV), the pH dependence (≈ -60 mV/pH unit) and the inhibition of this oxidation by DCMU (inhibitor of Q_A^- to Q_B electron transfer) are characteristics shared by a high-potential Photosystem II acceptor, Q_{400}, [11,12] discovered by Ikegami and Katoh [11] but not identified chemically. We have therefore attributed Q_{400}^+ to the Fe(III) state of the acceptor-side quinone-iron complex [10].

The most likely location of the iron is between Q_A and Q_B from magnetic coupling and structural arguments (analogy with the reaction centers of *Rhodopseudomonas viridis* [4]). This position would suggest that it plays a role in electron transfer from Q_A to Q_B. To explore this hypothesis further, originally proposed by Feher and Okamura [13] for bacterial reaction centers, we sought evidence for electron transfer from Q_A to the iron and from iron to Q_B. In this and the accompanying paper [14] we show that electron transfer does occur from Q_A^- to the Fe(III) and that a number of artificial quinones having $E_{m,7}(Q^-/QH_2) \geq E_{m,7}(\text{Fe(III)/Fe(II)}) - 60$ mV are capable of oxidizing the Fe(II) to Fe(III) by light-driven reduction-induced oxidation acting through the binding site of the secondary quinone, Q_B.

Material and Methods

Photosynthetic membranes. Thylakoid membrane fragments (BBY membranes) were prepared from market spinach with some modification [15,16] of the original procedure [17]. After the final centrifugation step, the membranes were resuspended at 6.5–12 mg Chl/ml in 10 mM Mes-NaOH (pH 6.2), 15 mM NaCl, 5 mM $MgCl_2$ and 0.4 M sucrose, frozen in liquid nitrogen and stored at $-80\,^\circ$C until use. For EPR measurements, samples were typically thawed and diluted to 3 mg Chl/ml with 3 mM Na_2-EDTA, 15 mM NaCl, 5 mM $MgCl_2$, 0.4 M sucrose plus 35–50 mM buffer: either Mes-NaOH (pH 5–6.5) or Hepes-NaOH (pH 6.8–8) or Ches-NaOH (8.5–9.5). For optical spectroscopy, the samples were diluted to 37 μg Chl/ml in the same medium, but without $MgCl_2$.

All exogenous quinones, at final concentrations ranging from 0.5 to 1 mM, were added from stock solutions in DMSO. The concentration of DMSO did not exceed 0.5% (v/v). An equivalent concentration of this solvent was added to all control experiments.

Optical spectroscopy. Optical spectroscopy mea-

surements were performed at 23 °C in a flash-detection spectrophotometer similar to that described by Joliot et al. [18]. Saturating actinic flashes were provided by a dye laser (Candela Co. Model SLL-150, 600 ns total duration with Oxazine 720, $\lambda_{max} = 693$ nm).

Electron spin resonance spectroscopy. The electron spin resonance spectrometer and cryostat were as described previously [10]. Except where otherwise stated, measuring conditions were as follows: $T = 4.2$–4.5 K, microwave frequency = 9.42 GHz, microwave power = 12.6 mW, modulation amplitude = 32 G.

Illumination of samples in EPR tubes (3 mm inner diameter was carried out in a transparent dewar containing a liquid-frozen acetone bath (200 K). Light was provided by a 360 W projector lamp, filtered by a 1.5 cm thick bath of saturated $CuSO_4$ (approx. 0.107 $J \cdot m^{-2} \cdot s^{-1}$). During illumination for a total of 3 min (four 90° rotations, 45 s each position), the sample temperature did not exceed 220 K.

In the light-induced Fe(II) oxidation experiments with exogenous quinones, the samples were first dark-adapted in the EPR tubes for 20 min at 10 °C. They were then frozen in the dark and their spectra recorded at 4.5 K. The samples were warmed to 200 K and illuminated as described above. After recording their spectra at 4.5 K, they were again reequilibrated at 200 K (in darkness) and then placed in an ice bath (0 °C) for 17 s in total darkness. The samples were again cooled to 4.5 K and their spectra recorded.

Results

Electron transfer from Q_A^- to Fe(III) – optical spectroscopy

BBY membranes were excited by saturating laser flashes (0.2 Hz, 600 ns duration, $\lambda_{max} = 693$ nm) and the resultant absorbance changes and their time courses were measured at 520, 540 and 550 nm. The difference $\Delta I/I$ at 550 minus that at 540 nm was used as a measure of the amplitude of C550, a local electrochromic indicator of the concentration of Q_A^- [19,20]. The measurements ($+K_3Fe(CN)_6$) at 520 nm and those at 540 and 550 nm in the presence of 20 μM DCMU ($\pm K_3Fe(CN)_6$) were used to correct for contributions of the field-indicating absorbance changes in

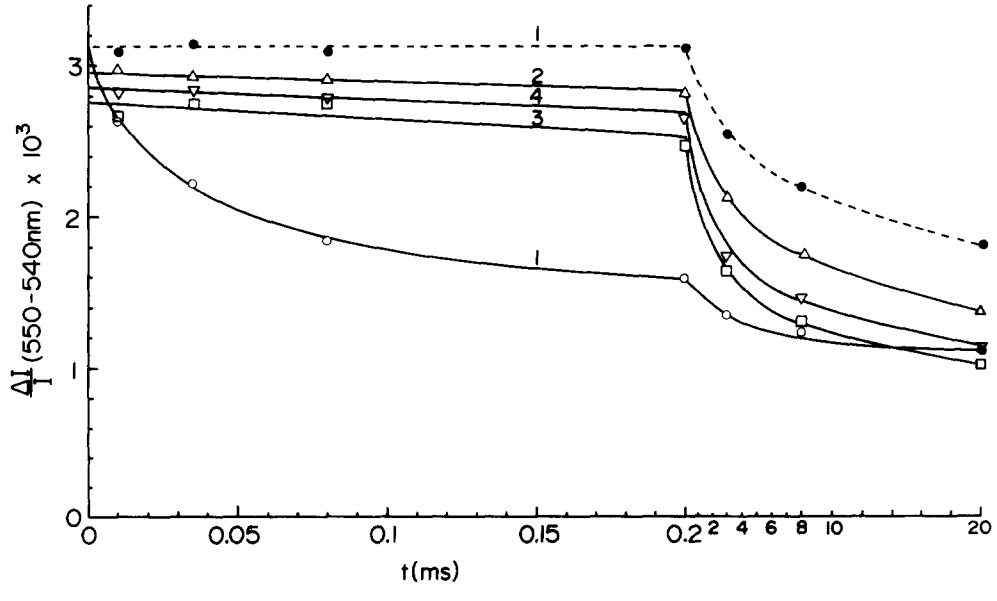

Fig. 1. Relaxation of C550 (Q_A^-, $\Delta I/I$ (550–540 nm)) after each of a number of saturating flashes (0.2 Hz) in the presence (open symbols) and absence (closed symbols) of 0.1 mM $K_3Fe(CN)_6$, pH 7.5 ($E_h \approx 470$ mV). Incubation time 30 min. Optical path length 16 mm. ●, no $K_3Fe(CN)_6$, first flash; ○, 0.1 mM $K_3Fe(CN)_6$, first flash; △, 0.1 M $K_3Fe(CN)_6$, second flash; □, 0.1 mM $K_3Fe(CN)_6$, third flash; ▽, 0.1 mM $K_3Fe(CN)_6$, fourth flash.

the 540–550 nm region at times up to 200 μs.

Fig. 1 shows that following 30 min incubation in the presence of 0.1 mM ferricyanide ($E_h \approx 470$ mV, pH 7.5, sufficient to oxidize fully the acceptor-side iron [10]), a fast phase appears in the relaxation of C550 which is not observed in the absence of oxidant. This fast phase, observed only on the first flash, relaxes with a $t_{1/2}$ of 25 μs, much faster than that of Q_A^- to Q_B electron transfer which occurs on the millisecond time scale in BBY membranes, as seen on subsequent flashes (Fig. 1). The initial amplitude of Q_A^- ($t < 10$ μs) in the presence of ferricyanide is also quite close to that observed in its absence.

These experiments show that Q_A^- is formed to the same extent in the primary charge separation, independent of the redox state of the acceptor-side iron. However, the lifetime of Q_A^- is greatly shortened by its oxidation in 25 μs by the Fe(III) present only on the first flash. Thus Q_A and the Fe(II) are located in series with the former being the first to receive an electron in the primary photoreaction. The equilibrium is very much toward reduction of the Fe(III) as one would predict from the relative midpoint potentials ($E_{m,7.5} \approx -30$ mV for Q_A/Q_A^- [21], 370 mV for Fe(III)/Fe(II) [10]). The reduction of the Fe(III) appears to be quantitative as it is observed only on the first flash. Reoxidation of the Fe(II) by ferricyanide, which requires minutes of incubation, does not occur between flashes. On the first flash, however, only half of the centers show the 25 μs relaxation. This may mean that there are centers which either lack Fe, or contain another metal in its place or, most likely, which are unable to have their Fe(II) oxidized (see below).

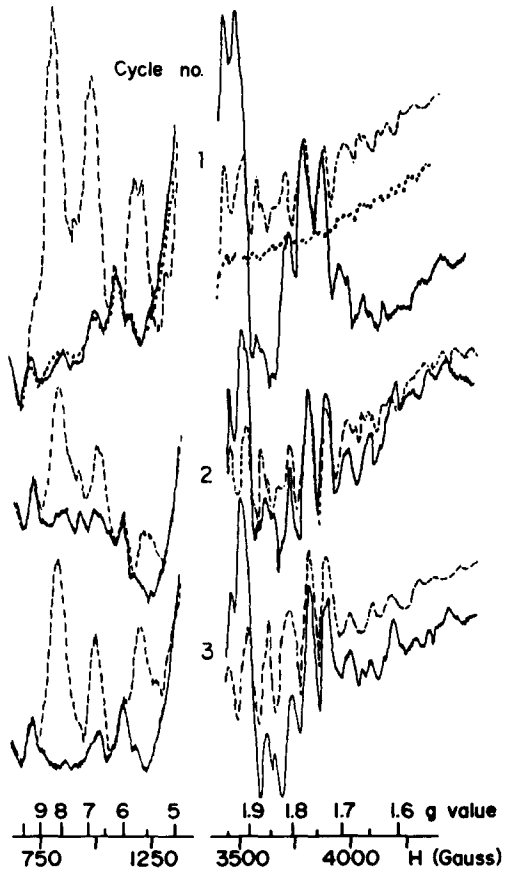

Fig. 2. Effect of three ilumination (200 K, 3 min): warming (0 °C, 17 s) cycles on the low-field Fe(III) signals (left) and the high-field Q_A^- Fe(II) signals (right) in the presence of 1 mM *p*-BQ at pH 7.0. The illumination warming and EPR detection conditions are as described in the Materials and Methods section, except that the spectra on the right were recorded at 31 mW microwave power and 25 G modulation amplitude. The gain was the same for all spectra.

Electron transfer from Fe(II) to secondary semiquinone – EPR spectroscopy

BBY membranes at pH 7.0 were dark-adapted for 20 min at 10 °C. After addition of 1 mM *p*-benzoquinone (*p*-BQ) in the dark, the sample was incubated for an additional 10 min at 0 °C and then frozen in an EPR tube in liquid nitrogen. The EPR spectrum was subsequently recorded at 4.4 K (Fig. 2, first cycle, dotted line). The sample was then warmed to 200 K and illuminated as described in the Materials and Methods section. The EPR spectrum, again recorded at 4.4 K (Fig. 2, first cycle, right, solid line) shows the appearance of a resonance at $g = 1.9$ and a broad minimum at $g = 1.65$, both of which are attributed to Q_A^--Fe(II) [9]. Warming of the sample, in the dark, to 0 °C for 17 s, followed by measurement at 4.4 K, gives rise to the spectrum of Fig. 2, first cycle, dashed lines. In this spectrum the Q_A^--Fe(II) signal has disappeared. New signals appear at low field having *g*-values of 8, 6.8 and 5.5. This spectrum is similar to the ones we have reported earlier [10] following addition of ferricyanide to membranes isolated form a mutant of *Chlamy-*

domonas lacking PS I and cytochrome b_6/f complex, and, with the exception of the resonance at $g = 6.8$ (see below), in BBY preparations. We attribute this spectrum to the PS II acceptor-side iron in the Fe(III) state.

If this sample is again illuminated at 200 K for 3 min, then the EPR spectrum recorded at 4.4 K (Fig. 2, second cycle, solid lines) shows the total disappearance of the low-field signals and the presence of a small $Q_A^-Fe(II)$ signal at $g = 1.9$. Warming the sample to 0 °C for 17 s (Fig. 2, second cycle, dashed lines) converts this small high-field signal to the same low-field signal observed following the first illumination-warming treatment, but of 3-fold smaller amplitude. Repetition of this propocol of illumination-warming treatment at 200 K, followed by warming to 0 °C, gives rise to an oscillatory behavior of period 2 of the $g = 1.9$ signal following illumination at 200 K and of the low-field signals following warming to 0 °C (Fig. 2). As shown in Fig. 3 for *p*-BQ (+) ad phenyl-*p*-BQ (○), these signals oscillate in synchrony and are maximal on odd-numbered cycles. Similar oscillations were observed for phenyl-*p*-BQ at pH 6.0. Control experiments at pH 7 showed no Fe(III) formation in the absence of added quinone.

We attribute this behavior to the following series of reactions:

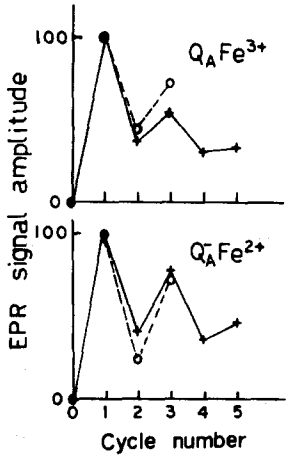

Fig. 3. Oscillation of the $Q_A^-Fe(II)$ signals ($g = 1.9$ and $g = 1.65$–1.7) following illumination at 200 K (bottom) and of the Fe(III) signals ($g = 5.5$–8) following warming in the dark to 0 °C (top) as a function of the cycle number. Same conditions as in Fig. 2, pH 7.0. +, *p*-BQ; ○, phenyl-*p*-BQ.

first cycle:

$$Q_AFe(II) \xrightarrow{h\nu} Q_A^-Fe(II) \overset{Q_{ex}}{\leftrightarrow} Q_AFe(II)Q_{ex}^-$$

$$\overset{2H^+}{\leftrightarrow} Q_AFe(III)Q_{ex}H_2 \leftrightarrow Q_AFe(III) + Q_{ex}H_2$$

second cycle:

$$Q_AFe(III) \xrightarrow{h\nu} Q_A^-Fe(III) \leftrightarrow Q_AFe(II)$$

third cycle: same as the first cycle.

The absence of Fe(III) following addition of quinone in the dark and its appearance upon single-turnover illumination of the reaction center indicates that it is the semiquinone which is the oxidizing species. While much of this work was done in parallel, this oscillatory behavior was first observed by Zimmerman and Rutherford [22] using saturating flashes at room temperature in the presence of phenyl-*p*-BQ. The intepretation given by these authors is in essential agreement with that reported here.

The oscillatory behavior described here is not perfect and there is loss of center synchrony with each cycle, resulting in a damping out of the oscillations. This is presumably due either to centers which have not undergone stable charge separation because of incomplete illumination or charge recombination (in competition with *p*-BQ reduction) or to centers which may have undergone double turnover, forming $Q_A^-Q_B^-$ upon illumination at 200 K on odd-numbered cycles or $Q_A^-Fe(II)$ on even-numbered cycles.

Following dark-adaptation for 20 min at room temperature, the Fe(II) reverts back to Fe(III). The centers are resynchronized and the full light-induced iron oxidation can again be observed on the first illumination-warming cycle.

Sources of donor-side electrons

The donor-side electrons come from several sources at 200 K (Fig. 4). On the first cycle the electron comes predominantly from the oxygen-evolving Mn-complex as evidenced by the large 'multiline' signal [23] corresponding to state S2 (two oxidizing equivalents stored, Fig. 4, left). The amplitude of this signal increases on the second cycle, probably due to centers initially in state S0

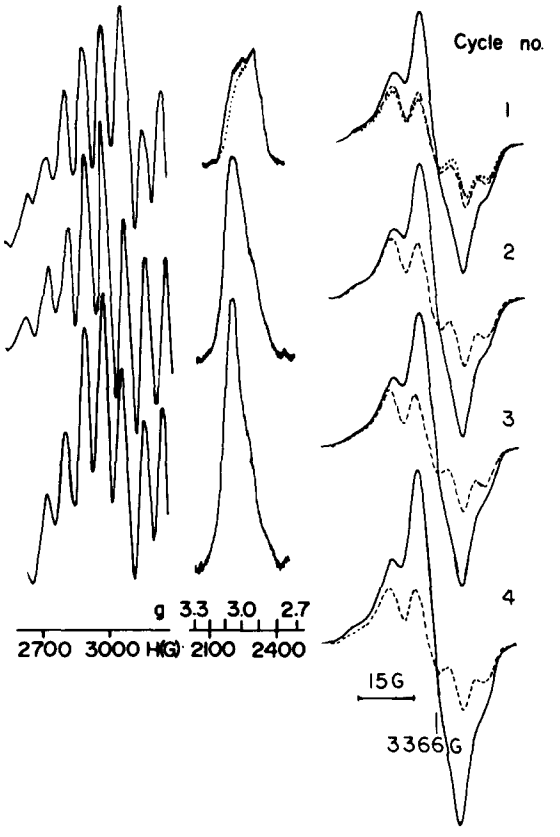

Fig. 4. Photosystem II donor-side EPR signals as a function of the cycle number during successive illumination-warming cycles. Conditions as in Fig. 2, except with 1 mM phenyl-*p*-BQ. Left: 'multiline' signal arising from the S2 state of the oxygen-evolving site. Right: $g = 2$ region showing Signal II and a narrow 10–11 G radical, probably arising from an oxidized chlorophyll cation. Continuous lines: spectra recorded after 200 K illumination. Dashed lines: spectra recorded after warming to 0 °C for 17 s. Where not shown separately, the dashed and continuous lines were superimposed. Dotted lines: initial dark-adapted signal level. EPR conditions: $T = 14$ K (50 K, right); microwave power = 12.6 mW (0.05 mW, right); modulation amplitude = 32 G (2 G, right); microwave frequency = 9.42 GHz.

in the dark. It decreases slightly on the third cycle and approx. 30% more on the fourth and fifth cycles (not shown) as a result of advancement to state S3 [24]. High-potential cytochrome *b*-559 (Fig. 4, middle) remains reduced throughout the first cycle. On cycles 2 and 3 there is an approximately equivalent increase in the oxidized form. No further increase occurs beyond the third cycle (not shown). Between illumination at 200 K and warming to 0 °C there is a small (approx. 15%, not shown) decrease in the amplitude of the oxidized high-potential cytochrome. In addition to the above, a narrow radical species at $g = 2$ (ΔH_{pp} = 10–11 G, Fig. 4, right) which while apparent on earlier cycles is particularly strong from the fourth cycle onward. This signal, analogous to one observed earlier in PS II reaction center particles devoid of an active oxygen-evolving site [25], probably arises from the oxidation of chlorophyll at 200 K when state S1 or reduced cytochrome *b*-559 are unavailable as electron donors. This signal disappears upon warming to 0 °C, probably by back reaction. This narrow free-radical is not observed on the earlier cycles if the quinone concentration is maintained below 0.6 mM. Its presence is probably attributable either to a low-level dark oxidation of cytochrome *b*-559 by quinone prior to illumination followed by its generation in the light or to light-induced electron transfer from antenna chlorophyll to exogenous quinone outside the reaction center.

It appears, then, that on the first three cycles, electrons are contributed at 200 K by the oxygen-evolving Mn-center and cytochrome *b*-559. These equivalents are not lost to charge recombination at 0 °C. From the fourth cycle onward, the narrow radical (10–11 G, probably Chl^+) is the dominant donor, the oxidizing equivalent of which is probably lost through back reaction upon warming to 0 °C. The limited net oxidation of the PS II donor side is undoubtedly the major contributor to the damping of the oscillations (Fig. 3).

Various high-potential p-benzoquinones show light-induced oxidation of Fe(II)

The photoreduction-induced oxidation of the Fe(II) can be observed under similar conditions to those of Fig. 2 using a variety of substituted *p*-benzoquinones (Fig. 5). We note that the light-induced EPR spectra of Fe(III) show somewhat different features with respect to each other and to ferricyanide oxidation in the region of $g = 5.2$–8. While not shown in Fig. 5, methyl-*p*-BQ at more than 2 mM shows an additional feature at $g = 7.2$, like that observed in the spectrum of 2,6-dimethyl-*p*-BQ at 1 mM (Fig. 5). These differences correspond to different symmetries for the Fe(II) in the presence or absence of these

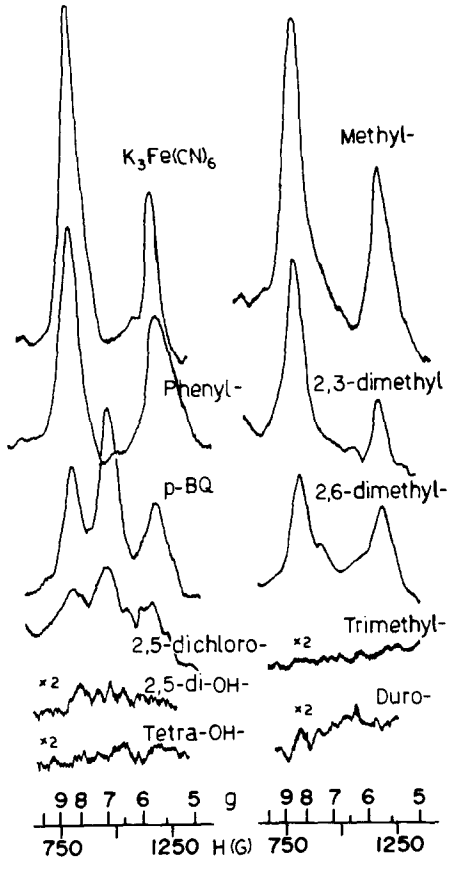

Fig. 5. Light-induced Fe(III) signals produced by a variety of substituted benzoquinones (1 mM) at pH 7.0 compared to those produced in the dark by 5 mM $K_3Fe(CN)_6$ ($E_h = 490$ mV). Conditions as in Materials and Methods. The quinone spectra are the difference between the 0 °C (17 s, dark) spectra and the 200 K (illuminated) spectra. The ferricyanide spectrum is the difference between that recorded after 50 min incubation at 0 °C and that following illumination of the sample at 200 K.

quinones, suggesting that their binding to the reaction enters modifies the Fe(III) environment.

As regards this point, we find that over 50% of the Fe(III) signal could be induced in samples containing 2 mM *p*-BQ or phenyl-*p*-BQ by dark adaptation for 2.5 min at 236–238 K following illumination at 200 K. In addition to weak $g = 5.5$ and 8 contributions, the *p*-BQ spectrum, which was the stronger of the two, consisted mainly of the $g = 6.8$ contribution, while that of phenyl showed a broad contribution at $g = 5.2$. Following subsequent dark adaptation for 20 s at 0 °C the $g = 5.5$ and 8 resonances more than doubled in size in both cases, while those at $g = 5.2$ (phenyl-*p*-BQ) and 6.8 (*p*-BQ) increased by only 15%. These observations indicate that both quinones are initially bound to over 50% of the reaction centers at 2 mM. This experiment implies that the Fe(III) signals at $g = 5.2$ and 6.8 would be due to Fe(III) centers with bound quinol. Bound quinone very likely shows these same signals, as the quinone form largely outnumbers the quinol in Fig. 5. We also show, in the accompanying paper (Fig. 5 in Ref. 14) that the spectrum for *p*-BQ in Fig. 5 (this paper) can also be observed in the presence of ferricyanide where no quinol is present.

Besides the differences in signal shape, the sig-

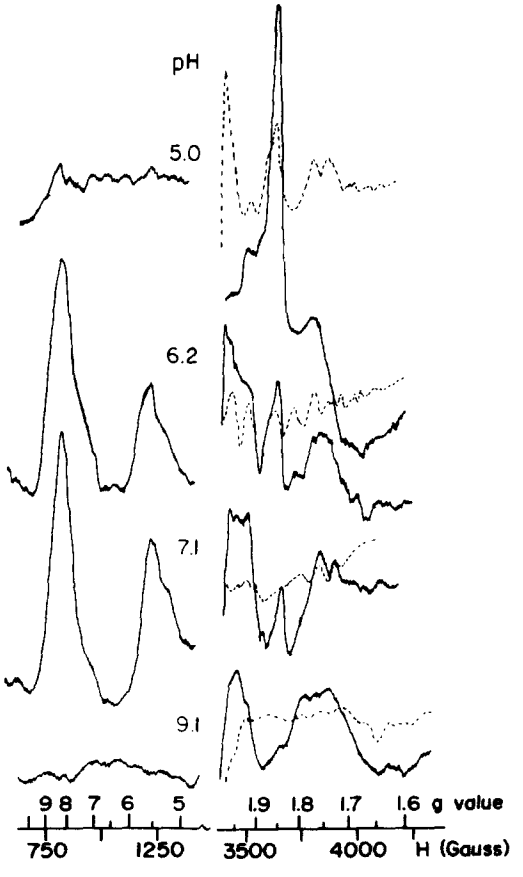

Fig. 6. Fe(III) (left) and the Q_A^- Fe(II) (right) signals obtained during a single illumination (200 K)-warming (0 °C) cycle at representative pH values in the presence of 1 mM phenyl-*p*-BQ. Left: 0 °C minus 200 K (illuminated) difference spectra. Right: solid line, after illumination at 200 K; dashed line, after warming to 0 °C in the dark.

nal area also varies significantly with the various quinones, indicating different extents of iron oxidation. Table I shows the midpoint potentials of most of these semiquinone/quinol couples in various states of protonation. We will see in the Discussion section that one of these couples, Q^-/QH_2, describes best the redox behavior we observe in Figs. 5 and 7.

pH dependence

Should the semiquinone anion be the species which oxidizes the Fe(II), one would predict that the net pH dependence of the light-induced oxidation would be -60 mV/pH unit, i.e., -120 mV for the Q^-/QH_2 couple and -60 mV/pH unit for the Fe(III)/Fe(II) couple. This pH dependence should prevail down to a pH where either all the Fe(II) becomes oxidized or where one attains the pK of the semiquinone (both resulting in a pH-independent region) or where one attains the pK of Fe(III) $(H^+) = Fe(III) + H^+$ (giving -120 mV/pH unit).

EPR signals for light-induced Fe(III) (Fig. 6, left) and Q_A^-Fe(II) (Fig. 6, right) in the presence of phenyl-*p*-BQ are shown in Fig. 6 at representative pH values. The pH-dependence of the signal size ((+), $g = 8$; (○), $g = 5.5$) is presented in Fig. 7. The light-induced oxidation peaks at pH 7.0 with 80% of the Fe(II) oxidized as compared to ferricyanide oxidation at this pH. The extent of light-induced oxidation falls off rapidly at both high and low pH. The behavior at high pH is consistent with the prediction of a net -60 mV/pH unit which implies that the pK of Fe(II) $(H^+) = Fe(II) + H^+$ is at least 9. The data are best fit by taking the $E_{m\,Q^-/QH_2}$ for phenyl-*p*-BQ equal to 455 mV. This value is lower than that estimated in Table I (496 mV). It is still probably an acceptable value in light of the lack of precise physicochemical data on this quinone. The rapid drop in the Fe(III) EPR signal as a function of pH below 7.0 is not predicted.

We have noted, in agreement with the earlier observation of Rutherford and Zimmermann [9] that as the pH is lowered, the position of the Q_A^-Fe(II) EPR resonance shifts from $g = 1.9$ to 1.84 (Fig. 6, right). We have also found that the relative ratio of the two resonance forms varies from preparation to preparation of BBY membranes, even at a given pH. If one plots the

TABLE I

VARIOUS REDOX COUPLES FOR SUBSTITUTED 1,4-BENZOQUINONES AT pH 7 FOR THE INDICATED STATES OF PROTONATION

Values for E^0_{Q/QH_2}, K_a, K_b, K_s and K_d, respectively, the standard potential for the Q/QH_2 couple, the first and second proton dissociation constants for the quinols, the proton dissociation constant for the semiquinones, and the stability constant for the latter were, with the exception of phenyl-*p*-BQ, taken from Rich and Bendall [30]. For phenyl-*p*-BQ, E^0_{Q/QH_2} comes from Flaig et al. [31]. The pK_a for this quinol was taken as 0.2 higher for phenyl- than for methyl- according to Ref. 31, but the reference value for methyl- was that of Ref. 30. K_s and K_d were assumed to be quite close to those for *p*-BQ in light of the similarity in the Hammett substituent constants for phenyl- and H- [32] and the first half-wave potentials for phenyl-*p*-BQ and *p*-BQ in acetonitrile [33]. While the second half-wave potential for phenyl-*p*-BQ is closer to that of methyl-*p*-BQ than *p*-BQ in the same solvent [33], the effect of ring substitution on the redox properties of substituted *p*-benzoquinones is smaller still in water than in acetonitrile.

Quinone	$E_{m,7}$ (mV)					
	Q/QH_2	QH/QH_2	QH/QH^-	Q^-/QH_2	Q^-/QH^-	Q^-/Q^{2-}
p-BQ	286	775	482	482	259	53
Phenyl-*p*-BQ	279	789	475	496	255	40
Methyl-*p*-BQ	230	727	412	445	196	−2
2,3-Dimethyl-*p*-BQ	174	701	390	425	126	−110
2,6-Dimethyl-*p*-BQ	174	692	350	419	127	−99
Trimethyl-*p*-BQ	115	654	279	386	68	−187
Tetramethyl-*p*-BQ	52	624	221	358	−2	−261
PQ-1	116	627	239	388	69	−186
UQ-1	76	621	191	382	22	−237
2,5-Dichloro-*p*-BQ	309	740	623	388	284	−157

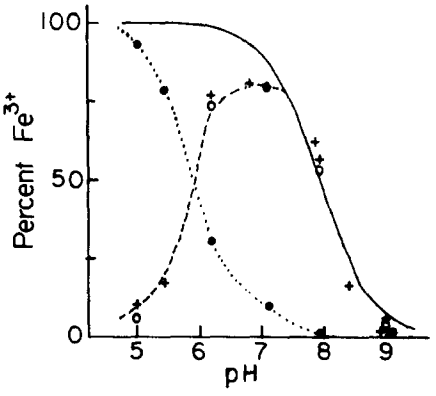

Fig. 7. pH dependence of the light-induced formation of Fe(III) in the presence of 1 mM phenyl-*p*-BQ. Illumination-warming conditions as in Fig. 2, (+) $g = 8$, (○) $g = 5.5$. The continuous line is a Nernst plot predicting the extent of oxidation of Fe(II). An $E_{m,7} = 400$ mV and a pH-dependence of -60 mV/pH unit were taken for the Fe(III)/Fe(II) couple. An $E_{m,7} = 455$ mV and a pH-dependence of -120 mV/pH unit were taken for the Q^-/QH_2 couple for phenyl-*p*-BQ. The 100% signal is that obtained upon full oxidation with ferricyanide. The dashed line is a corrected plot assuming that the amplitude of the light-induced $g = 8$ and $g = 5.5$ signals is inversely correlated with the amplitude of the $g = 1.84$ signal observed upon illumination at 200 K. The pH dependence of the latter is plotted as filled circles (dotted line).

relative amount of the $g = 1.84$ signal, formed upon illumination at 200 K, against the extent of the $g = 8$, Fe(III) signal, formed upon oxidation with ferricyanide at pH 7, then, among different preparations, one finds an anticorrelation between the two (not shown), with the extent of the $g = 8$ signal decreasing with increasing relative amounts of the $g = 1.84$. We also note in Figs. 6 and 7 that the decreased Fe(III) signal at low pH is paralleled by an increase in the $g = 1.84$ signal. The low pH variation of the $g = 8$ and $g = 5.5$ signals can be quantitatively accounted for (Fig. 7, dashed line) by a linear anticorrelation with the relative amount of the $g = 1.84$ signal. We conclude that the $g = 1.84$ signal most likely corresponds to a higher potential form of the Fe(II), not oxidizable by either $K_3Fe(CN)_6$ or phenyl-*p*-BQ.

Discussion

Electron transfer from Q_A^- to Fe(III)

We have recently shown [10] that the high spin Fe(II) of the quinone-iron acceptor complex of Photosystem II can be oxidized by ferricyanide to high-spin Fe(III). We have identified the acceptor-side iron with Q_{400}, a high-potential electron acceptor originally discovered by Ikegami and Katoh [11] through fluorescence measurements.

There exists rather contradictory evidence concerning the kinetics of Q_{400}^+ reduction by the reaction center [12,26–28], with half-times ranging from less than 300 ns [27] to 140 μs [26]. These estimations were based on measurements of fluorescence relaxation and induction and on double turnover of the PS II reaction center as revealed by the oxygen flash yield. It is also unclear from the earlier literature whether Q_{400} and Q_A are located in series or in parallel.

Using direct measurements of Q_A^- (C550) at pH 7 (Fig. 1), we have been able to show that Q_A and Q_{400}^+ (Fe(III)) are located in series with Q_A the first to receive an electron in the primary charge separation. Q_A^- subsequently transfers an electron to the oxidized acceptor-side Fe(III) with a $t_{1/2}$ of 25 μs at pH 7.5 (Fig. 1). It is likely that in PS II as in *Rps. viridis* reaction centers, Q_A and the Fe(II) are separated by a histidine imidazole, N-ligated to the Fe(II) [4]. The rapid electron transfer from Q_A to the Fe(III) is probably facilitated by the highly polarizable π-system of the imidazole or its low-lying non-binding orbitals [29].

Fig. 1 indicates that only half of the C550 relaxation is accounted for by the 25 μs phase following a first saturating flash in the presence of ferricyanide. Any positive contribution of Fe(II) minus Fe(III) to the $\Delta I/I$ (550–540 nm) would reduce the apparent extent of relaxation of C550, giving a constant off-set to the $\Delta I/I$ (550–540 nm) following a flash. At times greater than 200 ms (approx. 25% of the total signal), the relaxation occurs at the same rate after the first and subsequent flashes in the presence of ferricyanide (not shown). While the origin of this slow rate is not known (e.g., slow binding of PQ-9 to the Q_B site) any constant off-set on the first flash would have been apparent. We conclude that the contribution of Fe(II) minus Fe(III) to the $\Delta I/I$ (550–540 nm) is small (less than 25% of that of $Q_A^- - Q_A$) and that the 50% contribution arising from other than

the 25 μs phase on the first flash originates from centers in which the iron is either absent or in a non-oxidizable state (e.g., the = 1.84 form).

The rapid electron transfer from Q_A^- to Fe(III) was at least partially observed in the earlier experiments of Bowes and Crofts [26], who noted the appearance of a fast phase ($t_{1/2} = 140$ μs) in the relaxation of the fluorescence yield following a light flash at high redox potential. The fast phase was observed only following the first of a series of 20 ns saturating laser flashes. The discrepancy between our rate measurements and theirs could arise (a) partially from a difference in pH 7.5 here, 7.8 in Ref. 26) as the rate slows with an increase in pH, and more importantly, (b) from an underestimation of the rate due to a donor side quenching of the fluorescence yield at times up to 50 μs. An earlier estimation by Bowes et al. [12] of a Q_{400}^+ reduction rate of up to 5 μs could be explained in part by the lower pH (7.0) or possibly by a stimulation by Fe(III) of the quantum yield of formation of carotenoid triplet state, a fluorescence quencher.

The rate we report here is, however, quite consistent with the stimulation by ferricyanide of double oxidation of the oxygen-evolving site upon excitation of chloroplasts with a single 5–20 μs xenon flash [27,28]. Double-flash excitation [28] using non-saturating flashes, with oxygen detection on a third flash, gave an upper limit of 50 μs for the recovery of the center following a first photoreaction in the presence of ferricyanide. The limits for the rate of turnover would lie between 5 and 50 μs based on these oxygen measurements.

Light-induced oxidation of Fe(II) by exogenous quinones

Upon addition of exogenous quinones, we observe light-induced oxidation of Fe(II). That no such oxidation occurs in the dark indicates that it is the semiquinone and not the quinone which does the oxidation. Despite the differences in signal shape, one can compare, approximately, the extent of Fe(II) light-induced oxidation to the midpoint potentials at pH 7 of different semiquinone/quinol couples differing in the extent of protonation of the oxidized and reduced forms (Table I). The extent of Fe(III) formation follows most closely the E_m of the Q^-/QH_2 couple – note particularly the positions of *p*-BQ, 2,5-dichloro-, methyl-, 2,3-dimethyl- and 2,6-dimethyl-*p*-BQ in Table I and Fig. 5. Where the semiquinone is in the neutral form, the 2,5-dichloro-*p*-BQ is among the most oxidizing, unlike its position in Fig. 5 (about one-third of *p*-BQ). If the electron-transfer rate is determined by the free-energy change of the rate-limiting step [34], then the approximate correlation between the E_m and the extent of oxidation would suggest that the latter is not being limited kinetically by $QH \rightarrow QH^-$. While the observed trend is more consistent with $Q^- \rightarrow Q^{2-}$, the pH dependence at pH > 7 of the light-induced oxidation of the Fe(II) (Fig. 7) is indicative of an operating redox couple of Q^-/QH_2 (−120 mV/pH unit). The 17 s incubation, even though at 0 °C, is apparently long enough to allow full equilibration with protons. Actual studies of the rate of oxidation of Fe(II) by semiquinone as a function of pH will be required to identify the species actually doing the oxidation, whether Q^- or QH.

With the possible exception of tetramethyl- and phenyl-*p*-BQ, all the quinones have substituents which have Van der Waals radii (Cl: 1.8 Å; CH_3: 2.0 Å [35]) equal to or less than those of PQ-9 and should not be excluded from the Q_B binding site on steric grounds. That the extent of oxidation of the iron approximately agrees with the amplitude and relative positions of the E_m for Q^-/QH_2 would suggest that the effective midpoint potentials are the equilibrium potentials operating in solution and that the semiquinone is not bound to the Fe(II)-reaction center (RC) more tightly than the quinol to the Fe(III)-RC. The midpoint potential of the Q^-/QH_2 redox couple depends on the dissociation constants of both these species according to the following equation:

$$E_m(b) = E_m(f) + 2.303\frac{RT}{F}\log\frac{K_s}{K_q}$$

where $Q^- - RC \overset{K_s}{\leftrightarrow} Q^- + RC$ and $QH_2 - RC \overset{K_q}{\leftrightarrow} QH_2 + RC$ and where (b) ≡ bound, (f) ≡ free.

That tetramethyl-*p*-BQ produces some oxidation and trimethyl and PQ-9 (the natural acceptor) none at all could mean tighter binding of the semiquinone over the quinol in these cases, lowering the semiquinone/quinol midpoint potential.

The Fe(III) spectra differ in the presence of the different exogenous quinones, showing a resonance peak at $g = 6.8$ for *p*-BQ and 2,5-dichloro-*p*-BQ, and broader $g = 5$ resonances for some of the other quinones, compared with oxidation by ferricyanide. These different spectra suggest binding of the quinones close to the Fe(III) site, modifying the Fe(III) symmetry. That the binding site is indeed that of the secondary quinone, Q_B, will be shown in the accompanying paper [14] in which inhibitors, known to bind to the Q_B site, block the light-induced oxidation of the Fe(II).

The Fe(III) spectra observed in the presence of *p*-BQ and 2,5-dichloro-*p*-BQ using BBY membranes resemble that obtained with *Chlamydomonas* using ferricyanide alone [10]. In the latter case, an additional resonance was observed at $g = 6.4$, not observed in BBY membranes (Fig. 5) except upon addition of certain quinones or inhibitors which shift the EPR resonances to more axial positions. The Fe(III) environments thus differ between the two materials, possibly because of a higher binding affinity for plastoquinone in the presence of Fe(III) in the case of the *Chlamydomonas* membranes. In the accompanying paper [14], we will discuss further how molecules bound to the Q_B site might affect the shape of the Fe(III) spectrum.

Lavergne [36] has reported that the addition of benzoquinone to spinach chloroplasts, previously excited by a single saturating flash, showed rapid ($t_{1/2} = 100$ μs) reoxidation of Q_A^- on a second flash following the addition of 50 μM DCMU. Lavergne interpreted the fast Q_A^- reoxidation kinetics and the resistance to DCMU as an inability of the inhibitor to displace bound benzosemiquinone, the oxidant for Q_A^- on the second flash. The results presented here offer an alternative interpretation. Addition of benzosemiquinone, following the first flash, would have oxidized Q_B^- by the exogenous quinone. Indeed, Zimmermann and Rutherford [22] have shown this to occur for phenyl-*p*-BQ. The benzoquinone produced would then oxidize Fe(II) to Fe(III) forming the quinol. Addition of DCMU would have no effect on the Fe(III), allowing rapid electron transfer from Q_A^- to Fe(III) on the following flash. Considering that the pH at which Lavergne [36] worked (pH 8) is not an optimum for the light-induced oxidation of the iron (Fig. 7), the kinetics he observed were probably a combination of electron transfer from Q_A^- to the semiquinone in some centers and to Fe(III) in others.

pH dependence

We showed in Fig. 7 that there is a pH optimum for light-induced oxidation of Fe(II) by exogenous quinones. Zimmermann and Rutherford [22] have also presented preliminary evidence indicating a low yield of light-induced Fe(III) formation at low pH. In our hands the location of the pH optimum is not strict and has been observed to vary between pH 6 and 7, depending on the membrane preparation. While the behavior at pH values above the optimum is consistent with the redox properties of the Fe(III)/Fe(II) and Q^-/QH_2 couples, that on the low pH side is not. We note (Fig. 6), as reported by Rutherford and Zimmermann [9] that the form of Q_A^-Fe(II) changes from a *g*-value of 1.9 to 1.84 upon lowering the pH. The decreased ability to oxidize the Fe(II) using ferricyanide in preparations enriched in the $g = 1.84$ form would suggest that the anti-correlation between light-induced $g = 8$ formation and the $g = 1.84$ form of Q_A^-Fe(II) in Fig. 7 arises from the higher potential properties of the Fe(II) of the $g = 1.84$ centers. We cannot absolutely exclude that the binding affinity of the quinone or the semiquinone vs. the quinol forms could also depend on the state of the iron environment. However, after examining many BBY preparations, we have found that in those which show enrichment of the $g = 1.84$ form at pH 7, the Fe(II) is more difficult to oxidize, even by ferricyanide. This observation would tend to support a positive shift in E_m for the Fe(III)/Fe(II) couple in going from the $g = 1.9$ to the $g = 1.84$ state.

In the accompanying paper, we will exmaine more specifically the effect of PS II inhibitors on the Fe(III) signal and on the light-induced oxidation by exogenous quinones. These experiments provide conclusive evidence for electron transfer from Fe(II) to the exogenous quinones occupying the Q_B binding site. They show, as well, that the Fe(III) EPR signals are a sensitive probe of the binding interactions occurring between quinone and inhibitors and the amino acid side chains which line the Q_B pocket.

Acknowledgements

The authors would like to thank Drs. A. William Rutherford and Jean-Luc Zimmermann for their open and generous discussion of results of mutual interest during the course of this project and their making available a preprint of their work. We would also like to thank Dr. Antony Crofts who participated in the early stages of the optical spectroscopy measurements and who shared with us his insights on Q_{400}. We are also grateful to Drs. Klaus Brettel, Jérôme Lavergne, Peter Rich (and for his gift of 2,3-dimethyl-*p*-BQ), Stenbjørn Styring, Jean-Pierre Tuchagues and Bruno Velthuys for their valuable discussions and suggestions. We gratefully acknowledge as well the support of the CNRS contract no. 980029 and of an EMBO travel grant.

References

1 Nuijs, A.M., Van Gorkom, H.J., Plijter, J.J. and Duysens, L.N.M. (1986) Biochim. Biophys. Acta 848, 167–175
2 Bowes, J., Crofts, A.R. and Arntzen, C.J. (1980) Arch. Biochem. Biophys. 200, 303–308
3 Fowler, C.F. (1977) Biochim. Biophys. Acta 459, 351–363
4 Deisenhofer, J., Michel, H. and Huber, R. (1985) TIBS 10, 243–248
5 Butler, W.F., Calvo, R., Fredkin, D.R., Isaacson, R.A., Okamura, M.Y. and Feher, G. (1984) Biophys. J. 45, 947–973
6 Dismukes, G.C., Frank, H.A., Friesner, R. and Sauer, K. (1984) Biochim. Biophys. Acta 764, 253–271
7 Petrouleas, V. and Diner, B.A. (1982) FEBS Lett. 147, 111–114
8 Nugent, J.H.A., Diner, B.A. and Evans, M.C.W. (1981) FEBS Lett. 124, 241–244
9 Rutherford, A.W. and Zimmermann, J.L. (1984) Biochim. Biophys. Acta 767, 168–175
10 Petrouleas, V. and Diner, B.A. (1986) Biochim. Biophys. Acta 849, 264–275
11 Ikegami, I. and Katoh, S. (1973) Plant Cell. Physiol. 14, 824–836
12 Bowes, J.M., Crofts, A.R. and Itoh, S. (1979) Biochim. Biophys. Acta 537, 320–335
13 Feher, G. and Okamura, M.Y. in The Photosynthetic Bacteria (Clayton, R.K. and Sistrom, W.R., eds.), pp. 349–386, Plenum, New York
14 Diner, B.A. and Petrouleas, V. (1987) Biochim. Biophys. Acta 893, 138–148
15 Ford, R.C. and Evans, M.C.W. (1983) FEBS Lett. 160, 159–164
16 Rutherford, A.W., Zimmermann, J.L. and Mathis, P. (1984) FEBS Lett. 165, 156–162
17 Berthold, D.A., Babcock, G.T. and Yocum, C.F. (1981) FEBS Lett. 134, 231–234
18 Joliot, P., Béal, D. and Frilley, B. (1980) J. Chim. Phys. 77, 209–216
19 Knaff, D.B. and Arnon, D.I. (1969) Proc. Natl. Acad. Sci. USA 63, 963–969
20 Van Gorkom, H.J. (1974) Biochim. Biophys. Acta 347, 439–442
21 Diner, B.A. (1986) Encyclopedia of Plant Physiol., New Series, Vol. 19, Photosynthesis III (Staehelin, L.A. and Arntzen, C.J., eds.), pp. 422–436, Springer Verlag, New York
22 Zimmermann, J.L. and Rutherford, A.W. (1986) Biochim. Biophys. Acta 851, 416–423
23 Dismukes, G.C. and Siderer, Y. (1981) Proc. Natl. Acad. Sci. USA 78, 274–278
24 De Paula, J.C., Innes, J.B. and Brudvig, G.W. (1985) Biochemistry 24, 8114–8120
25 Nugent, J.H.A., Evans, M.C.W. and Diner, B.A. (1982) Biochim. Biophys. Acta 682, 106–114
26 Bowes, J.M. and Crofts, A.R. (1980) Biochim. Biophys. Acta 590, 373–384
27 Jursinic, P. (1981) Biochim. Biophys. Acta 635, 38–52
28 Velthuys, B.R. and Kok, B. (1977) Proceedings of the Fourth International Congress on Photosynthesis (Hall, D.O., Coombs, J. and Goodwin, T.W., eds.), pp. 397–407, The Biochemical Society, London
29 Isied, S.S. (1984) Prog. Inorg. Chem. 32, 443–517
30 Rich, P.R. and Bendall, D.S. (1980) Biochim. Biophys. Acta 592, 506–518
31 Flaig, W., Beutelspacher, H., Riemer, H. and Kälke, E. (1968) Liebigs Ann. Chem. 719, 96–111
32 Zuman, P. (1967) in Substituent Effects in Organic Polarography, pp. 273–308, Plenum, New York
33 Chambers, J.Q. (1974) in The Chemistry of the Quinoid Compounds (Patai, ed.), Ch. 14, Wiley Interscience, New York
34 Marcus, R.A. (1963) J. Phys. Chem. 67, 853–857
35 Gould, E.S. (1959) Mechanism and Structure in Organic Chemistry, p. 51, Hold, Rinehart and Winston, New York
36 Lavergne, J. (1982) Biochim. Biophys. Acta 679, 12–18